

Hyperpolarized ^{13}C MR imaging and corresponding histopathology for the non-invasive characterization of metabolism in the TRAMP model

K. R. Keshari¹, R. Bok², S. Sukumar², M. Van Criekinge², D. Vigneron², and J. Kurhanewicz²
¹UCSF, San Francisco, CA, United States, ²UCSF

INTRODUCTION: Hyperpolarized (HP) ^{13}C MR studies of the transgenic model of prostate cancer (TRAMP) model have demonstrated that [$1-^{13}\text{C}$]pyruvate can detect both local and metastatic prostate cancer, provide an assessment of pathologic grade [3], and early response to therapy [4]. Correlation of HP ^{13}C MR findings with pathologic stage, proliferation and hypoxia and how these correlate with current state-of-the-art multi-parametric imaging of prostate cancer is critical for understanding how well this model recapitulates the human situation and how HP ^{13}C MR might best be integrated into a clinical MR staging exam of prostate cancer. The combination of high field (14T) micro-imaging systems and DNP polarization provides the sensitivity necessary to obtain highly spatially and temporally resolved anatomic and functional imaging data for correlation with the HP ^{13}C MR data, pathologic data and immunohistochemical findings. The goal of this study was to develop and implement a 14T multi-parametric imaging protocol and compare the MR findings to histopathology and immunohistochemistry of normal and TRAMP mice at various stages of cancer progression in order to better understand the relationship between metabolism, pathology, diffusion, perfusion, hypoxia and proliferation.

METHODS: [$1-^{13}\text{C}$]pyruvate (14.2M) and ^{13}C urea (6.4M) were prepared using the OX063 radical and co-polarized using an Oxford HypersenseTM [5]. The experiments were performed on a 14T, 600WB micro-imaging spectrometer equipped with 100G/cm gradients (Varian Instruments). *In vivo* MR and *ex vivo* histopathology studies were performed on both normal (n = 3) and TRAMP (n = 3) mice. Multi-slice T_2 -weighted anatomic images were acquired using a respiratory-gated spin-echo sequence with a $T_E=20\text{ms}$, $T_R=1200\text{ms}$, fat saturation, FOV 40 x 40 mm, 256 x 256 points (RO x PE). Diffusion-weighted images were acquired using a spin-echo based sequence with similar parameters, 4 B-values (102, 305, 406, and 508) and apparent diffusion coefficient maps were calculated from fits of this data to a mono-exponential. An echo planar imaging (EPI) based pulse sequence was constructed using frequency-specific pulses (f = pyruvate, lactate or urea and $n, N=12$) to generate a 3D image for each metabolite with an acquisition time of approximately 180ms.

$$[90_f - (180_f - \text{EPI}_n)]_f$$

Data was zero-filled and transformed to a final resolution of 1.25mm isotropic (0.002cc). Average total carbon derived from pyruvate and urea were derived from a region of interest in the kidney and used to normalize the absolute signals in normal prostate and TRAMP tumors.

To understand the histopathology of normal prostate and TRAMP tumors relative to hyperpolarized imaging, prostate tissues were excised and stained using hematoxylin & eosin (H&E, for morphology), KI-67 (a nuclear stain for proliferation), and pimonidazole (PIM, a stain for hypoxia).

RESULTS AND DISCUSSION: Apparent diffusion coefficient (ADC) values are reduced 55% in the TRAMP tumors as compared to normal mouse prostate ($0.68 \pm 0.46 \times 10^{-3} \text{ mm}^2/\text{s}$ v. $1.47 \pm 0.59 \times 10^{-3} \text{ mm}^2/\text{s}$, $P < 0.005$ Figure 1), which is similar to the differences observed between human benign and malignant prostate tissues [6]. Representative ^1H T_2 -weighted images with overlaid HP ^{13}C 3D EPI images after injection of co-polarized [$1-^{13}\text{C}$]pyruvate and ^{13}C urea (Figure 1) demonstrate the distribution of ^{13}C urea and [$1-^{13}\text{C}$]lactate/[$1-^{13}\text{C}$]pyruvate in a normal (Figure 1a) and TRAMP mouse (Figure 1b). The average lactate-to-pyruvate ratio was significantly increased in TRAMP tumors relative to normal prostate (2.1 ± 1.7 v. 0.38 ± 0.13 , $P < 0.005$) similar to previously published results for moderate to late stage TRAMP tumors [3]. TRAMP tumors exhibited a significant increase in uptake of total HP pyruvate derived carbon ($1.23 \pm 0.89 \text{ AU}$ v. $0.86 \pm 0.22 \text{ AU}$, $P < 0.001$). Perfusion of the tumor was slightly elevated relative to normal prostate tissue ($0.77 \pm 0.51 \text{ AU}$ v. $0.66 \pm 0.15 \text{ AU}$, $P = 0.03$) though this had a large range, most likely a result of heterogeneous perfusion in the tumor. When comparing hyperpolarized data to histopathology, regions of necrosis demonstrated lack of HP signal (both HP urea, and HP pyruvate metabolites). At pathology, the late stage TRAMP tumors studied were >98% poorly differentiated as compared to 100% well-differentiation in normal prostate tissue (Figure 2). Normal prostate tissue stained 1% for KI-67 as compared to $88 \pm 6\%$ in the TRAMP tumors (Figure 2). Additionally, TRAMP tumors stained positive for PIM at $19 \pm 6\%$ as compared to <1% for normal prostate (Figure 2).

CONCLUSIONS: This study demonstrates the feasibility of acquiring high spatial resolution 14T multi-parametric MR data for correlation with both HP ^{13}C MR data and histopathology. Similar to the human situation, ADC is reduced in TRAMP tumors relative to normal prostate. Both increased proliferation and hypoxia were related to increased uptake of pyruvate and lactate-to-pyruvate ratio. Late stage TRAMP tumors had overall increased perfusion based on HP ^{13}C urea relative to the normal prostate. However, perfusion was heterogeneous within the tumor and there were regions of low perfusion with high metabolic activity. Ongoing studies include investigation of earlier stage TRAMP tumors to capture changes in hypoxia and proliferation as related to both hyperpolarized and standard MR parameters of early pathologic changes.

REFERENCES: [1] Golman K et al. Cancer Res 2003; 100(18): 10435-10439. [2] Ardenkjaer-Larsen J et al. PNAS 2003; 100(18): 10158-10163 [3] Albers MJ et al. Cancer Res 2008; 68(20): 8607-15 [4] Day S et al. Nat Med 2007; 13(11): 1382-7 [5] Wilson DW et al. J. Magn Reson 2010; 205(1) 141-7 [6] Noworolski S et al. Magn Reson Imaging 2008; 26(8): 1071-80 **ACKNOWLEDGEMENTS:** NIH R21 EB007588 and R21 GM075941-01, and the help of Kristin Scott.

Figure 1.

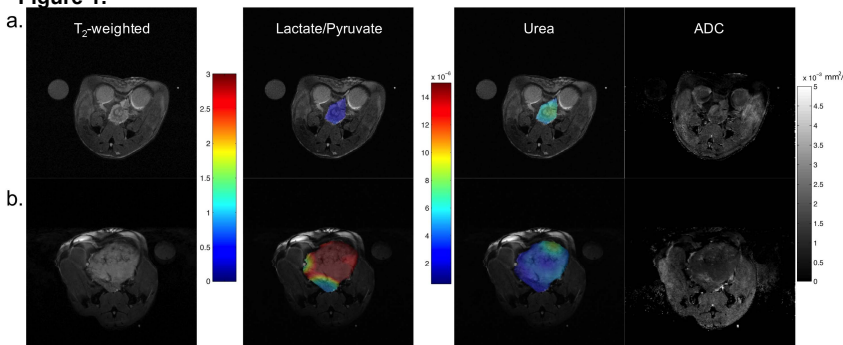


Figure 1. Representative T_2 -weighted images, ratio maps of [$1-^{13}\text{C}$]lactate to [$1-^{13}\text{C}$]pyruvate, hyperpolarized ^{13}C -Urea distribution and apparent diffusion coefficient (ADC) maps are shown for a normal prostate (a) and late stage TRAMP tumor (b).

Figure 2.

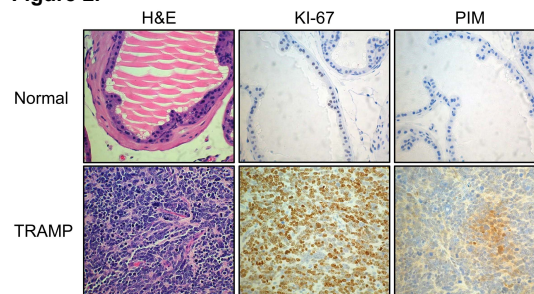


Figure 2. Representative histopathology from a normal mouse prostate and TRAMP tumor. High densities of poorly differentiated cells, proliferation and hypoxia are observed in the mid-late stage prostate tumor.